

OPTIMIZATION RESEARCH ON PLANT KEY PARAMETERS OF THE IMPELLER OF THE DUCTED NATURAL GAS PRESSURE POWER

by

**Ran ZHANG^{a,b}, Qian-Kun REN^{a*}, Han-Bing WU^a,
Cheng-Jun LV^a, and Yang LIAO^a**

^aSchool of Mechanical Engineering, Xihua University, Chengdu, China

^bState Key Laboratory of Oil and Gas Reservoir Geology and Exploitation,
Southwest Petroleum University, Chengdu, China

Original scientific paper
<https://doi.org/10.2298/TSCI2502101Z>

The impeller structure of the device is optimized based on the ducted natural gas pressure generation device. Based on the overall structure of the device, the numerical simulation model of the impeller is constructed by using FLUENT software. The optimal performance of 7° and 7 blades is obtained by taking the blade angle of attack and number as the optimization object, and the impeller speed and torque as the optimization object.

Key words: impeller structure, optimization design, numerical simulation

Introduction

Natural gas is transported over long distances by high pressure pipe-lines. In order to ensure the safe operation of the gas transmission network at all levels and the normal use of gas by users, the natural gas in the long-distance pipe-line can only be used after pressure reduction treatment [1]. Enormous pressure energy is released when high pressure natural gas is reduced to low pressure natural gas. It is very important how this pressure energy is utilized.

Principle of power generation device

High pressure natural gas driven by an expander generator to generate electricity is most of the existing natural gas pressure energy recovery methods [2]. However, the expander machine is mostly an external structure, the space required to install the equipment is large, and the multiple power loss of the connecting shaft is too large. Therefore, a new space-saving power generation method is proposed in this paper, and its structure principle is shown in fig. 1.

The high pressure natural gas shocks the impeller and causes it to rotate when natural gas enters from the differential pressure generator side. The impeller causes the rotor to rotate and the induction coil in the rotor produces an induced current in the stator winding as the rotor rotates.

Impeller design of power generation device

Taking a natural gas regulator station as an example, the inlet pressure is 0.4-0.8 MPa, the design flow is 1150 Nm³ per hour, and the rated output power of the power plant is 3 kW.

* Corresponding author, e-mail: 2540341247@qq.com

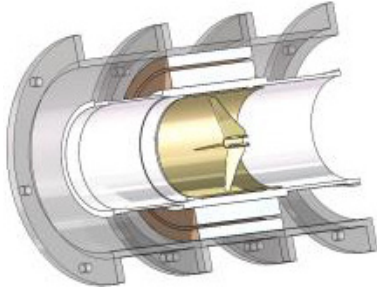


Figure 1. Structure principle of power generation device

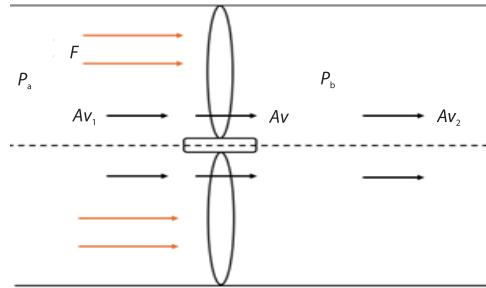


Figure 2. Diagram of an impeller under fluid action under ideal conditions

Limits of wind energy capture

Figure 2 is the schematic diagram of the impeller under the action of the fluid in ideal conditions. The axial force on the impeller:

$$F = m(v_1 - v_2) = \rho Av(v_1 - v_2) \quad (1)$$

where m is the fluid mass, v_1 – the fluid inlet velocity, v_2 – the fluid outlet velocity, ρ – the fluid density, and A – the impeller swept plane area.

From the pressure difference between the front and back of the impeller, the thrust expression of the axial impeller:

$$F = A(P_a - P_b) \quad (2)$$

where P_a is static pressure in front of impeller and P_b – the static pressure after impeller.

Substitute Bernoulli's equation into eq. (2):

$$F = 0.5\rho A(v_1^2 - v_2^2) \quad (3)$$

Thus:

$$v = \frac{v_1 + v_2}{2} \quad (4)$$

Define an axially induced induction coefficient a to describe the impeller's blocking effect on the fluid:

$$a = \frac{v_1 - v}{v_1} \quad (5)$$

The energy obtained by the impeller is the difference of the kinetic energy of the fluid-flowing through the impeller:

$$P = 0.5\rho A(v_1^2 - v_2^2) \quad (6)$$

Substitute v_1 and v_2 into the kinetic energy difference eq. (6):

$$P = 2\rho Av^3 a(1-a) \quad (7)$$

From the definition formula of wind energy capture coefficient C_p , it can be obtained:

$$C_p = \frac{P}{0.5Av_1^3} \quad (8)$$

By substituting P into the formula of wind energy capture coefficient (8), we can obtain:

$$C_p = 4a(1-a^2) \quad (9)$$

When $a = 1/3$, the wind energy capture coefficient reaches a maximum value of 0.593, which is called the Bates limit, and no impeller efficiency can exceed this limit value [3].

Impeller characteristic parameters

It can be obtained from the blade element theory:

$$v_L = \sqrt{(1-a)^2 v_x^2 + (1+b)^2 \omega^2 r^2} \quad (10)$$

where v_L is the operational wind speed, v_x – the relative wind speed, b – the tangential induction coefficient, ω – the impeller angular velocity, and r – the impeller radius.

The inflow angle:

$$\sin \varphi = \frac{v_x (1-a)}{v_L} \quad (11)$$

$$\cos \varphi = \frac{\omega r (1+b)}{v_L} \quad (12)$$

Angle of attack:

$$\alpha = \varphi - \beta \quad (13)$$

where α is the angle of attack, β – the pitch angle, and φ – the inflow angle.

The blade angle of attack is 4° according to the design working conditions [4, 5].

The blade tip speed ratio is an accurate reflection of the operating state of the turbomachinery under different wind speeds, which can be expressed:

$$\lambda = \frac{\omega r}{v_L} \quad (14)$$

The tip ratio can be calculated as 3 according to the working conditions[6].

In conventional applications, the number of blades must match the tip speed ratio of the impeller. The optimal number of blades is between 3 and 8 when the tip speed ratio is 3 [7].

Once the design power and design operational wind speed of the power generation device have been determined, the diameter of the impeller can be obtained:

$$D = \sqrt{\frac{8P_e}{\rho v_L^3 \pi C_p \eta}} \quad (15)$$

where P_e is the rated power of generator and η – the generator efficiency.

According to the design condition of the device, C_p can be estimated to be 0.38, and the impeller diameter, D , is 486 mm after calculation [8, 9].

The rated speed of the impeller is calculated in accordance with:

$$N = \frac{60 \lambda v_L}{\pi D} \quad (16)$$

The operational wind speed is 45 m/s, and the rated speed of the impeller can be calculated as 2300 rpm.

The selection of airfoil needs to be compared and analyzed with NACA4412 airfoil and RISØ-A-12 airfoil with high lift-to-drag ratio, and the airfoil with better aerodynamic shape is selected as the blueprint for appropriate modification and optimization [10].

Impeller structure optimization

A model comprising an impeller with a diameter of 500 mm, five blades, a blade pitch angle of 13°, a blade angle of attack of 5° and an inlet pressure of 0.5 MPa was employed for the purposes of simulation. Following stabilization, the rotor speed remained at 1600 rpm, exhibiting a discrepancy from the initial design index.

In order to enhance the overall power generation efficiency of natural gas pressurized power plant, a single variable research method was adopted to study the influence of blade attack angle and blade number on rotor performance.

Three groups of impellers with attack angles of 4°, 7°, 9° and other parameters unchanged were set up, and the optimal attack angle of the three groups of impellers was explored by simulation.

The torque and speed of the rotor in the fluid are important parameters to measure the rotor index. In order to explore the state of the impeller at different flow rates, the speed and torque changes of three groups of impellers with different attack angles at different flow rates are sorted out and compared to analyze the best working conditions of each blade. Figure 3 shows the curves of torque and speed of three types of impellers at different flow rates.

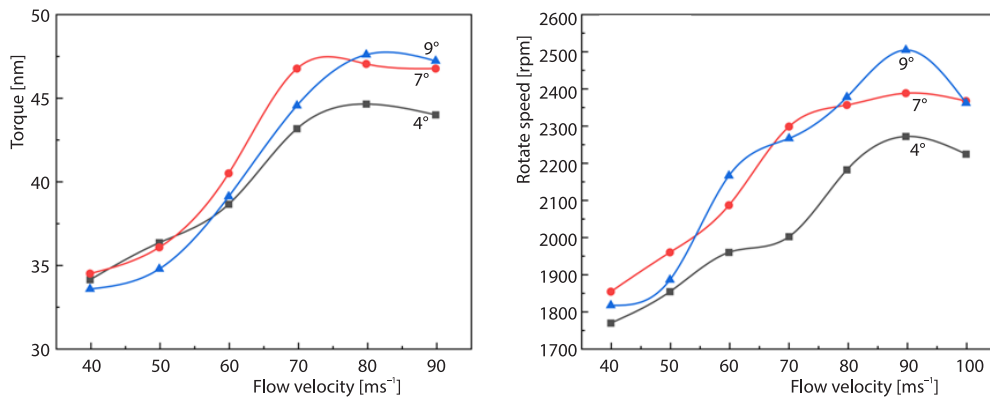


Figure 3. The 4°, 7°, and 9° of attack angle flow rate and torque, speed relationship

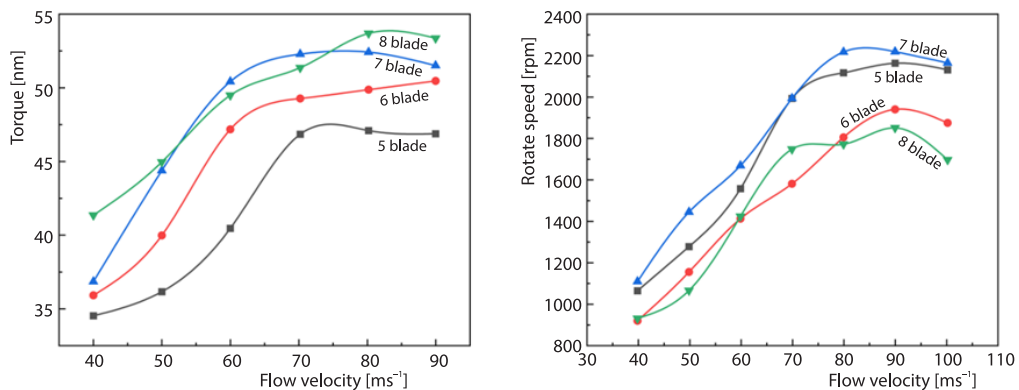


Figure 4. The 5°, 6°, 7°, and 8° vane impeller flow rate and torque, speed relationship

In conclusion, the 4° impeller demonstrates the least fluctuation in both rotation speed and torque value, however, its torque value is inferior to that of the 7° blade. The torque value

of the 7° impeller is notably high, with minimal fluctuations in speed. The torque value and speed of the 9° impeller exhibit the greatest fluctuations, with the speed displaying a state of oscillation that is detrimental to the stable generation of power by the motor.

Three models with the number of blades were set up, namely 5-blade, 6-blade, 7-blade, and 8-blade impellers, and other parameters of the impellers were kept unchanged. After sorting out the results of the four groups, the conditions of torque and speed at different flow rate are sorted into curves, as shown in fig. 4.

Overall, the number of blades is positively correlated with the torque and speed, among which the 7-blade impeller can maintain a higher maximum torque value and a larger stable operation range, so it is more suitable for this device.

Conclusion

In this paper, the impeller structure of the ducted natural gas pressure power plant is optimized, and its performance is improved by numerical simulation. The results show that the two parameters of blade attack angle and blade number are optimized, and the optimized blade attack angle and blade number are 7° and 7 blades, respectively, which can significantly improve the performance of the impeller.

Nomenclature

A – impeller swept plane area, [m²]
 a – axial induction coefficient, [-]
 b – tangential induction coefficient, [-]
 C_p – wind energy capture coefficient, [-]
 D – impeller diameter, [m]
 F – axial force, [N]
 m – fluid mass, [kg]
 N – operational wind speed, [rpm]
 P – kinetic energy obtained by the impeller, [J]
 P_a – static pressure in front of impeller, [Pa]
 P_b – static pressure after impeller, [Pa]
 P_e – rated power of generator, [W]
 r – impeller radius, [m]
 v – velocity of passing through the impeller, [ms⁻¹]

v_L – operational wind speed, [ms⁻¹]
 v_X – relative wind speed, [ms⁻¹]
 v_1 – fluid inlet velocity, [ms⁻¹]
 v_2 – fluid outlet velocity, [ms⁻¹]

Greek symbols

α – angle of attack, [°]
 β – pitch angle, [°]
 η – generator efficiency, [-]
 λ – blade tip speed ratio, [-]
 ρ – fluid density, [kgm⁻³]
 φ – inflow angle, [°]
 ω – angular velocity, [rads⁻¹]

Acknowledgment

The authors would like to express their gratitude to the Robotics Research Centre of Xihua University for its invaluable technical and financial assistance in conducting this study.

References

- [1] Brkovic, et al., Analysis of Loss Reduction in Natural Gas Transportation and Distribution, Energy Sources – Part B: Economics, Planning, and Policy, 10 (2015), 2, pp. 214-222
- [2] Kim, H., et al., A Study on Interconnecting to the Power Grid of New Energy Using the Natural Gas Pressure, Journal of Electrical Engineering & Technology, 15 (2020), 1, pp. 307-314
- [3] Coelho, P., The Betz Limit and the Corresponding Thermodynamic Limit, Wind Engineering, 47 (2023), 2, pp. 491-496
- [4] Suzuki T., et al., Analysis of Large-Scale Ocean Current Turbine Blades Using Fluid-Structure Interaction and Blade Element Momentum Theory, Ships and Offshore Structures, 5 (2018), 13, pp. 451-458
- [5] Go, J., Descriptions of Attack Angle and Ideal Lift Coefficient for Various Airfoil Profiles in Wind Turbine Blade, Journal of the Korean Society for Industrial and Applied Mathematics, 1 (2023), 27, pp. 75-86
- [6] Cui, X. H., et al., Effect of the Tip Speed Ratio on the Wake Characteristics of Wind Turbines Using LBM-LES, Energy Science Engineering, 4 (2024), 12, pp. 1638-1661

- [7] Yilmaz, O., Increasing Power Coefficient of Small wind Turbine over A Wide Tip Speed Range by Determining Proper Design Tip Speed Ratio and Number of Blades, *Proceedings of the Institution of Mechanical Engineers – Part C: Journal of Mechanical Engineering Science*, 23 (2022), 236, pp. 11211-11230
- [8] Hoffman, S.-M., *et al.*, Performance Characteristics of an Axial-Flow Gas Induction Impeller, *The Canadian Journal of Chemical Engineering*, 3 (2023), 101, pp. 1371-1386
- [9] Wekesa, D. W., *et al.*, Analytical and Numerical Investigation of Unsteady Wind for Enhanced Energy Capture in a Fluctuating Free-Stream, *Energy*, 42 (2017), 121, pp. 854-864
- [10] Elsayed, O. A., *et al.*, Induced Rolling Moment for NACA4412 Plain and Flapped Wing, *Aircraft Engineering and Aerospace Technology*, 1 (2010), 82, pp. 23-31